Current Research in MRI

Original Article

The Role of 3 Tesla Diffusion Weighted-Magnetic Resonance Imaging and Apparent Diffusion Coefficient Mapping with Aging and Gendering in Primary Parotid Tumors: Preoperative Foresight of Histopathological Subtypes

Abdurrahim Dusak[1], Adem Ağyar[1], Mustafa Çelik[2], Saime Shermatova[1], Veysel Kaya[1], Muhammed Emin Güldür[1]

[1]Department of Radiology, Harran University, Faculty of Medicine, Şanlıurfa, Turkey
[2]Department of Ear Nose & Throat, Harran University, Faculty of Medicine, Şanlıurfa, Turkey

Cite this article as: Dusak A, Ağyar A, Çelik M, Shermatova S, Kaya V, Güldür ME. The role of 3 Tesla diffusion weighted-magnetic resonance imaging and apparent diffusion coefficient mapping with aging and gendering in primary parotid tumors: Preoperative foresight of histopathological subtypes. *Current Research in MRI*. 2022;1(3):63-70.

The study has been presented at TNRD 2018 Congress as oral presentation.

Corresponding author: Abdurrahim Dusak, e-mail: adusak@gmail.com

Received: October 26, 2022 **Accepted:** December 26, 2022

DOI:10.5152/CurrResMRI.2022.221731

Abstract

Objective: Preoperative foresight of primary parotid tumors is decisive for surgical planning. We aimed to assign the role of 3 tesla diffusion-weighted magnetic resonance (3T DW-MR) imaging, apparent diffusion coefficient (ADC) mapping, aging, and gendering in differentiating the primary parotid tumor subtypes on the basis of histopathological correlation.

Methods: Thirty-one primary parotid tumors and tumor-free contralateral parotid glands of the same patients were evaluated retrospectively. The 3T DW-MR imaging, ADC, calculated apparent diffusion coefficient value, and demographic data were compared, and receiver operating characteristic analysis was carried out with histopathological results. A *P*-value <.05 was considered to be statistically significant.

Results: The apparent diffusion coefficient value of primer parotid tumors (n=31) was 1.43 ± 0.51 × 10^{-3} mm^2/s, of benign parotid tumors (n=25) was 1.61 ± 0.38 × 10^{-3} mm^2/s [Warthin tumors (n=7): 1.14 ± 0.20 × 10^{-3} mm^2/s, pleomorphic adenomas (n=18): 1.80 ± 0.24 × 10^{-3} mm^2/s], of malignant parotid tumors (n=6) was 0.69 ± 0.25 × 10^{-3} mm^2/s, and of normal parotid gland (n=31) was 0.94 ± 0.18 × 10^{-3} mm^2/s. Statistically, an intergroup differences was found between malignant and benign parotid tumors ($P < .001$). An intragroup difference was found between Warthin tumor and pleomorphic adenoma ($P < .001$). The results showed that aging and gendering were significantly different within primary parotid tumors ($P < .001$).

Conclusion: Using the results of 3T DW-MR imaging and ADC mapping with aging and gendering may provide preoperative primary parotid tumor characterization. The ADC value and age and gender might be useful in differentiating benign malign primary parotid tumors including subtypes such as Warthin tumor and pleomorphic adenoma. This aspect might be applied in routine applications.

Keywords: 3T DW-MR imaging, ADC mapping, primary parotid tumor, benign parotid tumor, Warthin tumor, pleomorphic adenoma, malignant parotid tumor

INTRODUCTION

The largest salivary glands and parotid gland have a specific structure; saliva is secreted through the parotid duct and digestion starts in the mouth.[1,2] Reports observed that parotid glands have a large variety of textures with aging and gendering and have a different histopathological subgroup of primary parotid tumors.[3-6] Pleomorphic adenomas display myxoid and chondroid matrices.[7] Adenoid carcinoma has myxoid, hyalinized, and mucinous matrices.[8] The management of parotid tumors needs a detailed figure of the histopathological processes affecting the parotid glands. While local residue and recurrence risk are high in pleomorphic adenomas (>80%), they are less in Warthin tumors (<5%) with regard to the same surgical procedure.[9,10] Determining a convenient surgical procedure for primary parotid tumors is not only a differential diagnosis between groups of malignant or benign parotid tumors but also a distinction of benign histopathological subgroups including Warthin tumor and pleomorphic adenoma.[8,11]

Image-guided fine-needle aspiration biopsy (IG-FNAB) is approved as a useful method for preoperative differential diagnosis, with cytopathological accuracy between 80% and 90% in primary parotid tumors.[10,12] IG-FNAB risk might be a potential inoculation, which can spearhead a higher possibility of local residue recurrence, particularly in malignant parotid tumors and pleomorphic adenomas.[8,11] The cytopathological differential diagnosis for several primary parotid tumors might be unfeasible or difficult.[9,10] Pleomorphic adenomas have a labile histopathological design

that could mimic adenoid and mucoepidermoid carcinomas.[13] By using IG-FNAB alone, the distinction between adenoma and adenocarcinoma is mostly impossible.[10]

Magnetic resonance (MR) imaging can identify the characteristics of primary parotid tumors and determine the contiguity and extension.[14,15] However, routine MR imaging cannot differentiate primary parotid tumors from histopathological subtypes by preoperative planning and operation procedure alone.[10-13] Diffusion-Weighted (DW) MR imaging, apparent diffusion coefficient (ADC) mapping, and calculated ADC values depict random molecular diffusion of the parotid gland and affect gland perfusion and salivating.[15-17] The adjustment b-factor is critical and decisive in determining ADC mapping. There is an inverse relationship between the ADC value and the b-factor. High b-factors are preferred to minimize the effect of the parotid gland.[18]

The parotid gland has a unique texture that increases fat accumulation and other chances of aging and gendering.[19,20] Primary parotid tumors contain complex tissues composed of myxomatous and lymphoid matrices and cystic and necrotic tissues.[3] Primary parotid tumors may not be homogeneous due to the presence of cystic areas, necrosis, degeneration, or bleeding.[9] Therefore, the evaluation of a large region of interest (ROI) in the myxomatous tumor might have misleading results in the primary parotid tumors.[21,22] DW MR imaging and ADC mapping can reveal biophysical disturbances associated with histopathological alterations in the tumoral process and might segregate with gantry strength.[23,24] To minimize this dilemma and achieve optimum image quality and tissue, characterization using 3 tesla (3T) DW-MR imaging with a 64-channel head and neck coil appears necessary.[3,18] Demographic data might be useful in distinguishing primary parotid tumors.[25] Benign parotid tumors are seen in younger patients, whereas Warthin tumor tendency is seen in elderly patients.[26] Gender was not dominant in the primary parotid tumors, while male predominance was shown in Warthin tumor.[5] In the current study, we investigated 3T DW-MR imaging and ADC mapping using aging and gendering of the benign and malign primary parotid tumor and common subtypes of benign parotid tumors such as Warthin tumor and pleomorphic adenoma with histopathological correlation and to check our data with previous literary instructions.

MAIN POINTS

- The largest salivary glands and parotid gland have a specific structure. Parotid glands have a large variety of textures with aging and gendering and have a different histopathological subgroup of primary parotid tumors.
- Management of parotid tumors needs a detailed figure of the histopathological processes affecting the parotid glands. While local residue and recurrence risk are high in pleomorphic adenomas (>80%), they are less in Warthin tumors (<5%) with regard to the same surgical procedure.
- The apparent diffusion coefficient (ADC) value of pleomorphic adenoma was significantly higher than that of Warthin tumor and malignant parotid tumor. The ADC value of Warthin tumor was lower than that of the pleomorphic adenoma and higher than that of the malignant parotid tumor. By aging in pleomorphic adenoma was lower when compared to Warthin tumor and malign parotid tumor, and gendering in Warthin tumor was male dominance when compared to pleomorphic adenoma and malign parotid tumor. 3 Tesla DW-MR imaging and ADC mapping with aging and gendering might be useful in differential diagnosing of malignant and benign parotid tumors including Warthin tumors and pleomorphic adenomas.

METHODS

The institutional ethics committee approved our study (date: July 5, 2018, Session: 07, Decision: 18.07.24). Our medical study had retrospective consideration and was administered following the Helsinki Declaration. Moreover, this research was approved by the corporate ethics board. Thirty-one patients (20 females, 11 males; mean age 43 (18-81) years) who had primary parotid tumors were included. The study group consisted of patients with operated primary parotid tumors. The control group was established as contralateral normal parotid glands of the same patients. The exclusion criteria were poor MR imaging, simple cyst, and metastatic parotid tumors. The 3T-DW MR imaging of patients was performed between 2016 and 2018. The study was conducted at Şanlıurfa Harran University Hospital Radiology Department.

Magnetic Resonance Imaging Protocol

Each patient with a primary parotid tumor underwent MR imaging using the 3T MR scanner system (Magnetom Skyra, Siemens Healthcare, Erlangen, Germany) and using a 64-channel phasedarray head and neck coil. Routine MR imaging was performed with T1-weighted (T1W) (Time to Repetition (TR): 300 ms, Time to Echo (TE): 2 ms, Flip Angle (FA): 70°), T2W (TR: 4930 ms, TE: 91 ms, FA: 180°), turbo spin echo (tse), and fat saturation (fs) T1W (TR: 822 ms, TE: 13 ms, FA: 160°) images in the axial and T2W (TR: 4150 ms, TE: 37 ms, FA: 160°) tse images in the coronal plane. After an intravenous injection rate of 3 mL/s of 0.1 mmol/kg Gadobutrol (Gadovist; Bayer Schering Pharma, Berlin, Germany) fs T1W (TR: 822 ms, TE: 13 ms, FA: 160°) axial and T1W (TR: 300 ms, TE: 2 ms, FA: 700) sagittal and coronal images were obtained. 3 Tesla DW MR imaging (TR: 6400 ms, TE: 98 ms, FA: 90°, number of excitations (nex: 1, interslice: 0.5 mm, field: 22 × 22, thickness: 5 mm, matrix: 128 × 128) was obtained in an axial plane using an echo-planar Spin Echo (SE) sequence with a b value of 1000 mm^2/s tracing on conventional MR imaging. The acquisition time for 3T DW-MR images was 46 s.

Magnetic Resonance Imaging Processing and Data Analysis

Apparent diffusion coefficient mapping was generated from 3T DW-MR images for each patient, and ADC values were calculated manually by using the ellipsoid ROI for the appropriate placement of the primary parotid tumor and the contralateral normal parotid gland, in the same patient with routine MR image guiding, excluding cystic and necrotic areas. The ADC value from the contralateral normal gland was calculated in the same patient from the control group. For each measurement of parotid tumor and normal parotid glands, the ROI was placed at 4 mm^2 as symmetrically as possible except for intra-parotid lymph nodes and retromandibular vein.

Histopathological Analysis

After 3T DW-MR imaging, histopathological examinations were handled for the primary parotid tumors that were surgically resected to support definitive histopathological data in all patients. An experienced pathologist (M.E.G.) evaluated all surgical resection specimens. Histopathological subtypes of the primary parotid tumors (n=31) were benign parotid tumors (n=25), including Warthin tumor (n=7), pleomorphic adenoma (n=18), and malignant parotid tumor (n=6), including mucoepidermoid carcinoma (n=2), squamous cell carcinoma (n=2), non-Hodgkin lymphoma (n=1), and leiomyosarcoma (n=1).

Statistical Analysis

The obtained ADC values of the primary parotid tumor and contralateral normal parotid gland from all patients were evaluated by the Shapiro–Wilk normality test to see whether ADC values showed normal distribution. One-way analysis of variance (ANOVA) and post-hoc least significant difference test (Tukey) were used for normal distributed data. The data were recorded as mean ADC value ± SD. Whether the data were normally distributed or not was evaluated with the Shapiro–Wilk test. For comparisons between the 2 groups, normally distributed parameters were evaluated with the Student's *t*-test and non-normally distributed parameters were evaluated with Mann–Whitney *U* test. For comparisons between more than 2 groups, normally distributed parameters were evaluated with 1-way ANOVA and non-normally distributed parameters were evaluated with Kruskal–Wallis *H* test. Results were expressed as the mean difference and *P*-value. Differences among the ADC values and demographic data for malign and benign parotid tumors, within common benign parotid tumors including Warthin tumor and pleomorphic adenoma, and normal parotid gland were evaluated using 1-way ANOVA. If the *P*-value was significant, a multiple comparison test was used to determine the differences between groups. We averaged the ADC value of primary parotid tumors and healthy parotid glands of each patient. Statistical analyses were performed with Statistical Package for the Social Sciences version 23.0. (IBM SPSS Corp.; Armonk, NY, USA) . 3 Tesla DW MR image analysis was implemented independently by 2 head and neck radiologists (A.D. and V.K.). The difference between malignant and benign primary parotid tumors and common benign subtypes of Warthin tumor and pleomorphic adenoma was investigated, and the threshold value was determined using receiver operating characteristic (ROC) analysis. Statistically significant value was accepted as $P < .05$.

RESULTS

Thirty-one primary parotid tumors [7 Warthin tumors, 18 pleomorphic adenomas, 6 malignant parotid tumors (2 mucoepidermoid carcinomas, 2 squamous cell carcinoma, 1 non-Hodgkin's lymphoma, and 1 leiomyosarcoma)] and 31 contralateral normal parotid gland were included in the current study.

The calculated ADC values (Table 1) for histopathologically confirmed primary parotid tumors were demonstrated as follows; the primary parotid tumor: $1.43 \pm 0.51 \times 10^{-3}$ mm²/s, the benign parotid tumor: $1.61 \pm 0.38 \times 10^{-3}$ mm²/s [Warthin tumor: $1.14 \pm 0.20 \times 10^{-3}$ mm²/s (Figure 1) and pleomorphic adenoma: $1.80 \pm 0.24 \times 10^{-3}$ mm²/s (Figure 2)], the malignant parotid tumor: $0.69 \pm 0.25 \times 10^{-3}$ mm²/s (Figure 3); and the contralateral normal parotid gland: $0.94 \pm 0.18 \times 10^{-3}$ mm²/s.

Table 1. ADC Mapping of Primary Parotid Tumors

Groups	n	Gender	Age (Years)	ADC Value (Mean ± SD)
Primer parotid tumor	31	20 male/11 female	42.9 ± 16.1 (18-81)	1.43 ± 0.51 × 10^{-3} mm²/s
Benign parotid tumor	25	16 male/9 female	39.2 ± 14.5 (18-76)	1.61 ± 0.38 × 10^{-3} mm²/s
Warthin tumor	7	7 male/0 female	55.0 ± 12.8 (39-76)	1.14 ± 0.20 × 10^{-3} mm²/s
Pleomorphic adenoma	18	10 male/8 female	33.1 ± 09.8 (18-50)	1.80 ± 0.24 × 10^{-3} mm²/s
Malign parotid tumor	6	4 male/2 female	58.3 ± 13.7 (42-81)	0.69 ± 0.25 × 10^{-3} mm²/s
Normal parotid gland	31	20 male/11 female	42.9 ± 16.1 (18-81)	0.94 ± 0.18 × 10^{-3} mm²/s

ADC, apparent diffusion coefficient.

The age distribution of the primary parotid tumor was 42.9 ± 16.1 (18-81) years, of the benign parotid tumor was 39.2 ± 14.5 (18-76) years (Warthin tumor: 55.0 ± 12.8 (39-76) years, pleomorphic adenoma: 33.1 ± 9.8 (18-50) years), and of the malign parotid tumor was 58.3 ± 13.7 (42-81) years.

Gender dispersion of the primary parotid tumor demonstrated a male predominance, as the male-to-female ratio was 20/11, that of the benign parotid tumor was 16/9, that of Warthin tumor was 7/0, that of pleomorphic adenoma was 10/8, and that of the malign parotid tumor was 4/2.

Box plots of ADC mapping of primary parotid tumors and individual aging are shown in Figure 4.

ADC mapping in the primary parotid tumor (Table 2), we found that pleomorphic adenoma had significantly higher ADC value than Warthin tumors ($P < .001$) and malign parotid tumors ($P < .001$). Warthin tumor had a higher ADC value and a statistically significant difference than malign parotid tumor ($P = .007$). The normal parotid gland has a significantly lower ADC value than the pleomorphic adenoma ($P < .001$). Nevertheless, the normal parotid gland ADC value was lower than the Warthin tumor ($P = .176$) and higher than malignant parotid tumors ($P = .146$) but not statistically significant and hence indistinguishable.

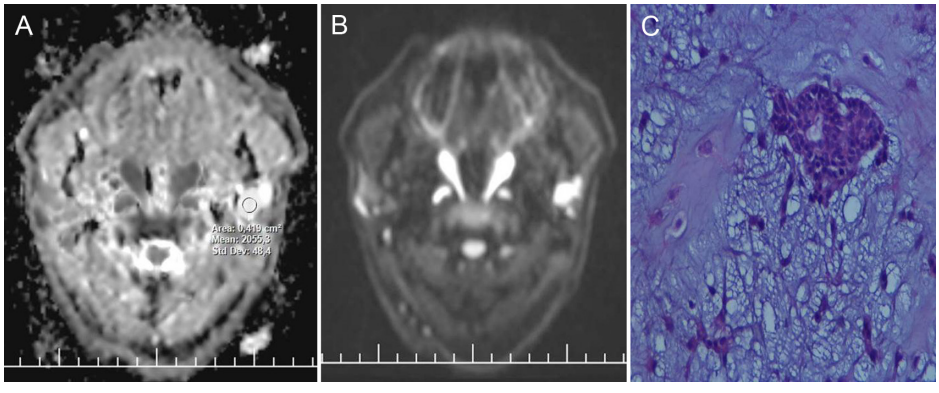

Figure 1. A 42-year-old female with left parotid pleomorphic adenoma. A–C, benign parotid tumor located in deep lobe tumor on axial 3T DW-MR image (A) and ADC mapping (B) and histopathological image (C) myoepithelial cells without atypia are observed on myxoid ground (HE, ×400).

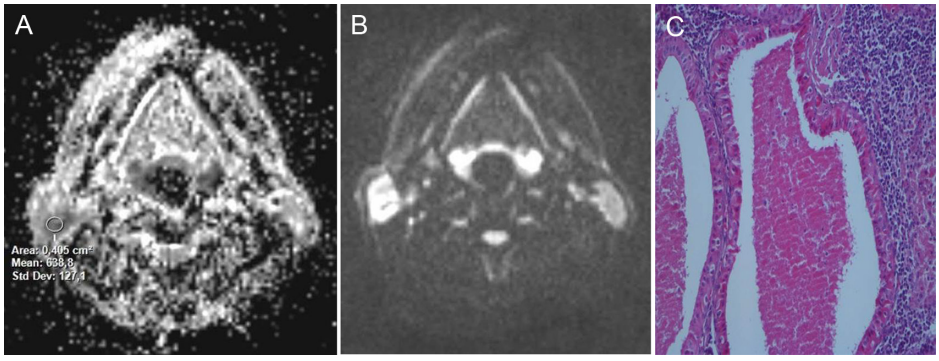

Figure 2. A 69-year-old male with right parotid Warthin tumor. A–C, benign parotid tumor located in superficial lobe on axial 3T DW-MR image (A) and ADC mapping (B) and histopathological image (C) lymphoid stroma, cystic structures covered with oncocytic cells and eosinophilic secretion in the cyst lumen (HE, ×200).

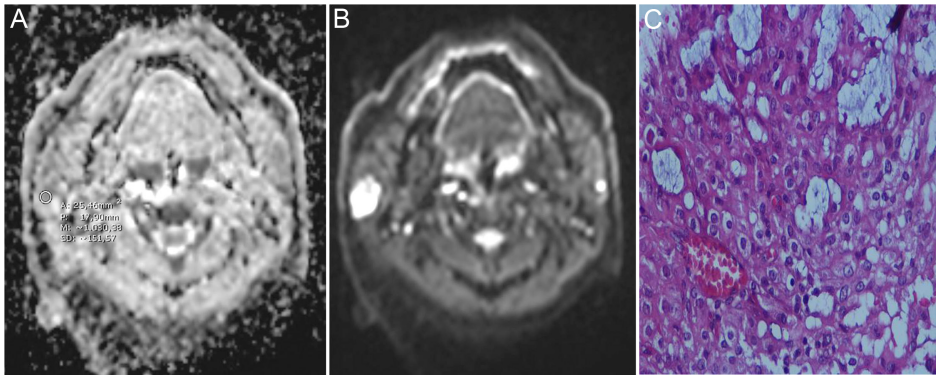

Figure 3. A 58-year-old female with right mucoepidermoid carcinoma. A–C, located in right superficial lobe malignant parotid tumor on axial 3T DW-MR image (A) and ADC mapping (B) and histopathological image (C) mucin-containing tumor tissue consisting of atypical epithelial cells is observed (HE, ×400).

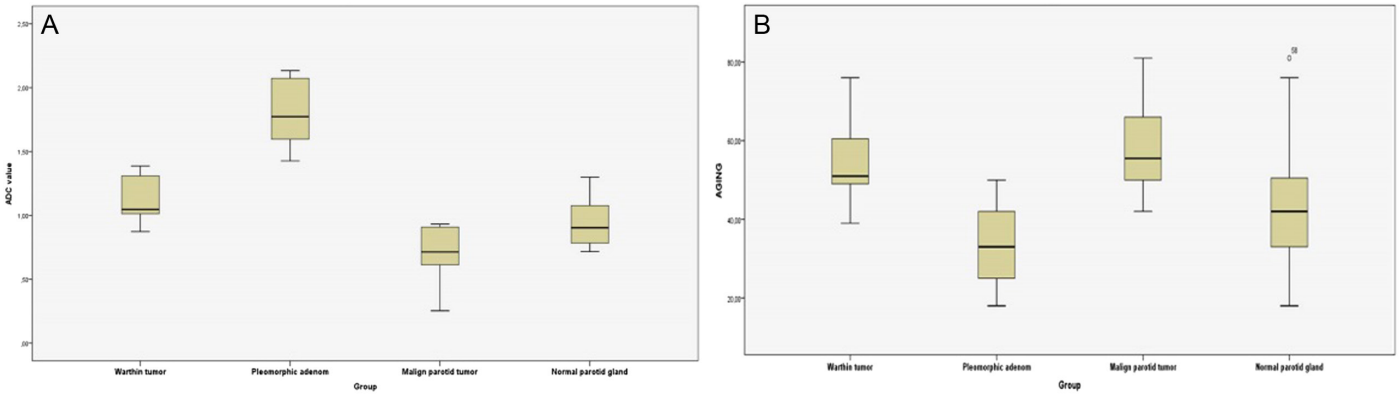

Figure 4. Box plots of apparent diffusion coefficient value (A) and ageing (B) associated with primary parotid tumors: Warthin tumor, pleomorphic adenoma, malignant parotid tumor, and normal parotid gland.

Table 2. Intergroup ADC Comparisons, Post-Hoc Test

Groups	Benign Parotid Tumor	Warthin Tumor	Pleomorphic Adenoma	Malign Parotid Tumor	Normal Parotid Gland
Primer parotid tumor					<0.001
Benign parotid tumor				<0.001	<0.001
Warthin tumor			<0.001	0.007	0.176
Pleomorphic adenoma		<0.001		<0.001	<0.001
Malign parotid tumor	<0.001	0.007	<0.001		0.146

Table 3. Intergroup Age Comparison, Post-Hoc Test

Groups	Benign Parotid Tumor	Warthin Tumor	Pleomorphic Adenoma	Malign Parotid Tumor	Normal Parotid Gland
Primer parotid tumor					<0.001
Benign parotid tumor				0.028	0.667
Warthin tumor			<0.010	0.980	0.243
Pleomorphic adenoma		0.010		0.004	<0.141
Malign parotid tumor	0.028	0.980	0.004		0.117

Table 4. Primary Parotid Tumors, ROC Analysis Between Each Groups

ADC value	Cutoff Value	Sensitivity	Specificity	PPV	NPV	AUC	95% CI
Primer parotid tumor and normal parotid gland	0.93	80	61	67	76	0.79	0.67-0.92
Benign parotid tumor and malign parotid tumor	0.96	96	100	86	100	0.99	0.95-1.00
Pleomorphic adenoma and Warthin tumor	1.41	100	71	90	100	1.00	1.00-1.00
Pleomorphic adenoma and primer parotid tumor	1.37	100	63	62	100	1.00	1.00-1.00
Warthin tumor and primer parotid tumor	0.93	100	72	46	100	0.80	0.57-1.00
Malign parotid tumor and primer parotid tumor	0.96	96	100	40	92	0.98	0.95-1.00
Benign parotid tumor and normal parotid gland	1.34	80	100	91	88	0.93	0.87-1.00
Pleomorphic adenoma and normal parotid gland	1.36	100	100	100	100	1.00	1.00-1.00
Warthin tumor and normal parotid gland	0.98	86	65	35	95	0.76	0.57-0.95
Malign parotid tumor and normal parotid gland	0.75	67	81	40	92	0.78	0.56-0.96

ADC, apparent diffusion coefficient; AUC, area under the curve; NPV, negative predictive value; PPV, positive predictive value; ROC, receiver operating characteristic.

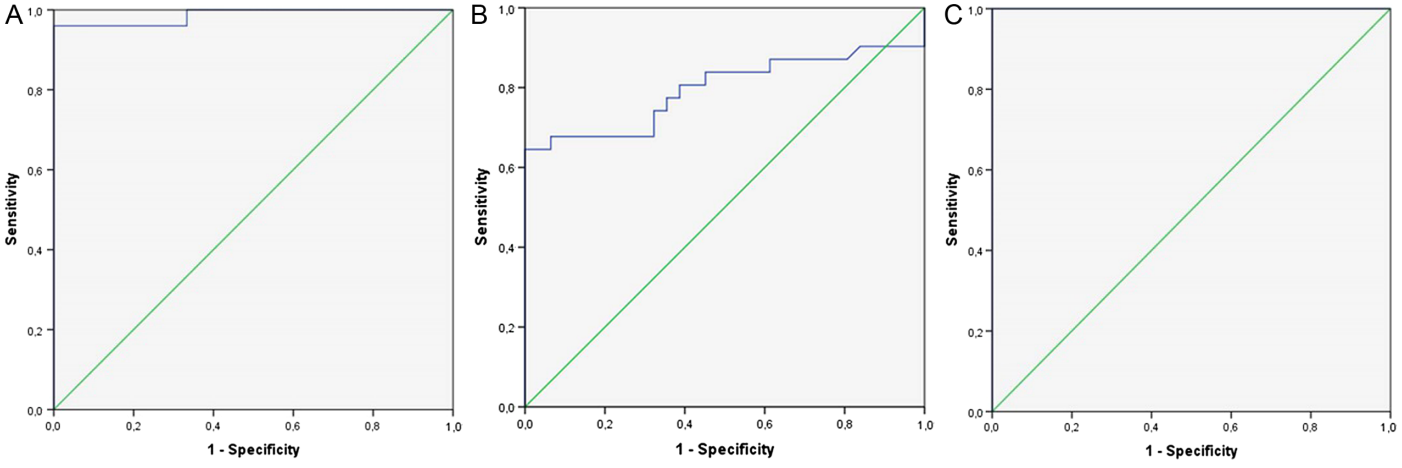

Figure 5. Receiver operating characteristic analysis graphs in primary parotid tumor—normal parotid gland (A), benign parotid tumor—malignant parotid tumor (**B**), and Warthin tumor—pleomorphic adenoma (C).

With aging in the primary parotid tumor (Table 3), we found that the age of the malign parotid tumor was higher than that of the benign parotid tumor ($P = .028$) and the age of the Warthin tumor was higher age than that of pleomorphic adenoma ($P < .010$).

Gendering in the primary parotid tumor, Warthin tumor had a higher male predominance than pleomorphic adenoma and malign parotid tumor.

Using the distinction performance of ROC analysis in the diagnosis of primary parotid tumors was appreciated. The sensitivity, specificity, positive and negative predictive value, area under the curve (AUC), and 95%CI were evaluated (Table 4). The cutoff value for benign and malignant parotid tumors was 0.96×10^{-3} mm^2/s and that for Warthin tumor and pleomorphic adenoma was 1.41×10^{-3} mm^2/s. The 95% CI) was 0.95-1.00. Sensitivity and specificity were 96% and 100%, respectively, and positive and negative predictive values were 86% and 100%, respectively (Figure 5). Interobserver correlation for 3T DW-MR imaging and ADC mapping was high (0.96 intraclass coefficient).

DISCUSSION

Among all organs, the parotid gland is the organ with the largest tumor subgroup histopathologically. Tumors often originate from the parotid gland. Salivary gland tumors constituted 3%-12% of head and neck regional tumors and 2%-3% of tumors that can be observed in the whole body.[1] Also, parotid gland tumors are 80% of salivary gland tumors.[27] The most common benign parotid tumors are Warthin tumors and pleomorphic adenoma.[28] The possibility of the primary parotid tumor is 1 of these 2 tumors that should be considered first.[11,29] Pleomorphic adenoma tends to be seen in younger patients than Warthin tumors and malignant parotid tumors.[5] Pleomorphic adenoma is well-circumscribed, encapsulated, and slightly lobulated, containing myxoid, mucoid, and chondroid matrices which provide prominent hyperintense and hypointense heterogenous areas due to the epithelial component on T2W-MR

imaging.[8,23] Pleomorphic adenoma contains various textures, including secretory glands, epithelium, and surrounding fatty stroma.[7] Glandular areas in adenoma and adenoid group tumors can consist of fluid deposits. Causatively, protons move freely in fluid accumulation areas and reflect a high ADC value in pleomorphic adenoma.[16,30]

We peruse the role of 3T DW-MR imaging and ADC mapping in recognizing primary parotid tumor histopathological subtypes. Our study showed that there was a prominent distinction between malignant and benign parotid tumors and within Warthin tumor and pleomorphic adenoma. Pleomorphic adenoma had a higher ADC value than Warthin tumor, malignant parotid tumor, and normal parotid gland. Warthin tumor and malignant parotid tumor might be nearly isointense, indistinguishable from a normal parotid gland on ADC mapping. Aging and gendering might be associated with increasing recognition of primary parotid tumors. The core of our outcomes from this study is using aging and gendering ADC mapping might be a prominent foresight in the differential diagnosis of primary parotid tumors.

The parotid gland has a unique and inhomogeneous texture, which consists of the interstitium and salivary components, and has shown extensive individual variety and changes with aging and gendering.[6,9] The parotid gland indicates a decreasing ADC value due to increased fat aggregation.[19] In a recent study, malignant parotid tumors and the Warthin tumors had been reported to appear isointense to the normal parotid gland on ADC mapping.[9] However, The ADC value of the malignant parotid tumor was lower than the normal parotid gland and the ADC value of the benign parotid tumor and the Warthin tumor was higher than normal parotid gland but it was not statistically significant in our study.

In another study, a small proportion of pleomorphic adenoma was reported to exhibit a typical shiny hyperintensity.[7,16] Nevertheless, primary parotid tumors cannot be diagnosed using routine MR imaging properties.[10,16] Warthin tumor is inclined to be seen in older patients than pleomorphic adenoma with a male predominancy.[5] Warthin tumor is well-edged, unencapsulated, and lobulated, with cystic components and colloid matrices.[30] Warthin tumor consists of rich lymphoid areas, germinal centers, and prominent follicles and exhibits hypercellularity, higher microvesselling, and micronecrotic changes.[3] Hypointensity on DW-MR imaging and ADC mapping is usually observed in the Warthin tumor as well as in malignant parotid tumors.[16,17] No significant difference was observed between Warthin tumor and malignant parotid tumors, so there was overlapping with ADC mapping in most of the study.[1,16]

Malignant parotid tumors can be histopathologically diagnosed according to mitotic activity, cellular anaplasia, necrosis, and neural invasion.[31] Malign parotid tumors, including lymphoma, carcinoma, and carcinosarcoma or mixed tumors, exhibit hypercellularity and limited proton diffusion space of extracellular fields, as a result of restricted DW-MR imaging.[23] Malignant parotid tumors, such as adenoid cystic carcinoma and mucoepidermoid carcinoma, indicate an increased signal intensity reflecting the cystic component due to mucin secretion.[8,17] Malignant parotid tumors exist lower ADC values than Warthin tumors; and also benign parotid tumors exist lower ADC values than Warthin tumors.[5] Cystic carcinoma and pleomorphic adenoma had higher ADC values and overlapping.[10] Therefore, most authors reported that ADC mapping could not discriminate between benign and malignant parotid tumors.[8,16] Carcinosarcoma is a mixed malignant primary parotid tumor, an extremely rare but important subgroup of malignant parotid tumors characterized by reproducing from pleomorphic adenoma or primarily de novo.[32,33] In contrast to these findings, ADC mapping of malignant parotid tumors was lower than benign parotid tumors in our study, and there was no overlap between malignant and benign parotid tumors.

Lymphoma, which forms an important subgroup of malignant parotid tumors, is characterized by diffuse and abundant infiltration of anaplastic lymphoid cellular in the germinal center and conspicuous follicles.[16,34] The ADC value of lymphoma is lower than carcinomas.[5,17] Lymphoma grouped in malignant parotid tumors with carcinomas in our series has a low ADC value. Therefore, lymphoma and malignant parotid tumors with low ADC values can be distinguishable from benign parotid tumors, including Warthin tumors and pleomorphic adenoma. The ADC mapping of malignant parotid tumors was lower than benign parotid tumors in our study, and there was no overlap between malignant and benign parotid tumors. By the way, we demonstrate that ADC mapping is helpful and can differentiate benign and malignant parotid tumors.

Management of primary parotid tumors is complicated due to their diversity, complex structure, various histopathological subgroups, and even subgroups exhibiting different biological behaviors.[4,11] Preoperative evaluation and deciding the appropriate surgical procedure requires a high-diagnostic technique.[20,33] Routine MR imaging is useful in differential diagnosis and frequently encounters distinctive morphological features.[16,22] Benign parotid tumors and also pleomorphic adenoma markedly hyperintense heterogeneous in T2W-MR imaging.[7,13] Warthin tumors with excess cystic components might resemble pleomorphic adenoma, and smaller cystic components might mimic malignant parotid tumors.[5] Heterogeneous hypointensity with contour irregularity might be facilitates diagnosis in malignant parotid tumors.[1,5] Preoperative differential diagnosis of a primary parotid tumor is important in terms of preoperative surgical planning.[11,35] Benign primary parotid tumors such as Warthin tumors and pleomorphic adenomas are excised with lobectomy, and subtotal parotidectomy, but malign parotid tumors are resected by total parotidectomy.[16,36]

MR imaging assists in determining the signal intensity, boundary, laterality, plurality, location, extension, and invasion of adjacent muscular and fascial parapharyngeal planes and facial nerve for surgical resection planning in primary parotid tumors.[16,34] Magnetic resonance imaging is widely used to differentiate malignant parotid tumors with irregular and vague margins, extraglandular extension, and accompanying lymph nodes.[2,30] Inhomogeneity and hypointensity of T2W MR imaging mostly suggest malignant parotid tumors, but it not sufficient to differentiate diagnosing them alone.[11,23] A benign parotid tumor might be an inhomogeneous nautre resembles malignant parotid tumors.[8] Therefore, the precise diagnosis of a primary parotid tumor with various histopathological subgroups cannot be situated by MR imaging.[1] Contrast-enhanced MR imaging could be used with diagnostic success, but using gadolinium has become lessened in recent years, and there is a need to develop new MR techniques without gadolinium.[1,14]

DW-MR imaging as a functional MR imaging modality might be provide qualitative and quantitative evaluation by demonstrating random movement of protons in a microtexture in routine without gadolinium.[1,16] DW-MR imaging in head and neck have susceptibility artifacts and impaired imaging, swallowing, and movement.[4,14] Using a 3T MR imaging system and a 64-channel head and neck coil with shorter imaging time and higher resolution, it is possible to obtain the optimal

DW-MR imaging and ADC mapping and calculate the ADC value of the parotid gland and primary parotid tumor.[18-24] The ADC value increases with respect to increasing fluid content in the primary parotid tumor.[16] Cystic and necrotic areas and pure cystic tumors might be excluded from ROI, to reflect the histopathology of the primary parotid tumor, and solid areas might be mapped and measured.[10,30] In a recent study, a lower ADC value reflects restricted proton movement in highly cellular areas of Warthin tumors.[5,16] However, in the aforementioned study, the authors included the whole tumor including necrotic cystic areas in the ROI.[3] As we defined, we excluded the cystic necrotic area from ROI to avoid variable ADC mapping. In agreement with these findings, the ADC value of the Warthin tumor was higher than that of the malignant parotid tumors. Therefore, we found that ADC mapping was useful to discriminate benign parotid tumors, including Warthin tumors, from the malignant parotid tumor. In a recent study, the ADC value of malign parotid tumor, Warthin tumor, and pleomorphic adenoma were reported as a $1.04 \pm 0.35 \times 10^{-3}$ mm^2/s, $0.97 \pm 0.35 \times 10^{-3}$ mm^2/s, and $1.74 \pm 0.37 \times 10^{-3}$ mm^2/s.[16] The ADC value in benign parotid tumor was $1.50 \pm 0.48 \times 10^{-3}$ mm^2/s and in malignant parotid tumor was $1.07 \pm 0.29 \times 10^{-3}$ mm^2/s.[23] In a recent study, the primary parotid tumors suggest isointense with normal parotid gland without distinguish of differantial diagnosis.[9] We revealed a little higher ADC value for the Warthin tumor ($1.14 \pm 0.23 \times 10^{-3}$ mm^2/s). Moreover, Warthin tumor has a propensity lower ADC value than pleomorphic adenoma, and higher than the malign parotid tumor. In agreeing with these findings, ADC mapping of the malignant parotid tumor and Warthin tumor was not significantly different from the normal parotid gland we studied. Even so, we noticed that ADC mapping might be helpful to differentiate malign from benign parotid tumors and Warthin tumor and pleomorphic adenomas but not from the normal parotid gland. Using 3T DW-MR imaging and 64-channel head and neck coil, to compose the ADC mapping and using aging and gendering might be useful in differentiate diagnosing from malignant and benign parotid tumors and Warthin tumor and pleomorphic adenoma.

Study Limitations

Our study has several limitations. First, there were limited primary parotid tumors, and therefore only a small number of subgroups of primary parotid tumors were included in the study, but smoking status was not addressed. We included Warthin tumors, pleomorphic adenomas, and malignant primary parotid tumors because malignant parotid tumors were few and heterogeneous, and it is not possible to identify 3T DW-MR imaging and ADC mapping in each subgroup statistically. Second, primary parotid tumor location, growth patterns, margins, signal intensity, cystic and necrotic content, and contrast enhancement were not evaluated, because this study was designed on standard head and neck MR imaging and focused on 3T DW-MR imaging ADC mapping. Thirdly, 3T DW-MR imaging ADC mapping was organized with b-values of 500-1000 sc/mm^2, higher b-values (2000-3000 sc/mm^2) might improve the study. However, there were several studies with conflicting results, and the first report was on qualitative and quantitative evaluation of primary parotid tumors using age, gender, and histopathological data using 3T DW-MR imaging and ADC mapping to characterize primary parotid tumors.

Further prospective studies must be carried out with a high number and wide histopathological subgroup of primary parotid tumors, and this evaluation method of primary parotid tumors using a cutoff value is expected to be an indicator of the distinction of the primary parotid tumor subgroups. Consequently, this research study can aid the relevant literatüre and implies for future research and via emphasizing the 3T DW-MR imaging and ADC mapping, together with aging and gendering, on the distinction of malignant and benign parotid tumors and subgroups, which should be addressed in routine primary parotid tumor imaging protocol.

CONCLUSIONS

In conclusion, our results suggested that 3T DW-MR imaging and ADC mapping with aging and gendering could prominently improve the distinction of malignant and benign parotid tumors including Warthin tumors and pleomorphic adenomas. The ADC mapping of pleomorphic adenoma was significantly higher than that of Warthin tumor and malignant parotid tumor, but the ADC value of Warthin tumor was lower than that of the pleomorphic adenoma and higher than that of malignant parotid tumor. Aging in pleomorphic adenoma was lower when compared to Warthin tumor and malign parotid tumor, gendering in Warthin tumor was male dominance than pleomorphic adenoma and malign parotid tumor. It indicated that the 3T DW-MR imaging and ADC mapping with aging and gendering might be useful in differential diagnosing of malignant and benign parotid tumors, including the Warthin tumors and pleomorphic adenomas.

Ethics Committee Approval: The institutional ethics committee has approved for our study from Şanlıurfa Harran University Hospital Radiology Department (Date: July 5, 2018, Decision No: 07).

Informed Consent: Written informed consent was obtained from patients who participated in this study.

Peer-review: Externally peer-reviewed.

Author Contributions: Concept – A.D., M.C.; Design – M.C., A.A.; Supervision – A.D., V.K.; Resources – A.D., M.C.; Materials – S.S., M.E.G.; Data Collection and/or Processing – A.D., A.A.; Analysis and/or Interpretation – V.K., S.S.; Literature Search – S.S., A.A.; Writing Manuscript – A.D., A.A.; Critical Review – M.D., V.K., M.E.G.

Declaration of Interests: The authors declare that they have no conflictsinterest.

Funding: The authors declare that this study has received no financial support.

REFERENCES

1. Karaman CZ, Tanyeri A, Ozgur R. Parotid gland tumors: comparison of conventional and diffusion weighted MR imaging findings with histopathological results. *Turk J Radiol*. 2017;36:60-68.
2. Sumi M, Takagi Y, Uetani M, et al. Diffusion-weighted echoplanar MR imaging of the salivary glands. *AJR*. 2002;178(4):959-965. [CrossRef]
3. Eida S, Sumi M, Sakihama N, Takahashi H, Nakamura T. Apparent diffusion coefficient mapping of salivary gland tumors: prediction of the benignancy and malignancy. *AJNR Am J Neuroradiol*. 2007;28(1):116-121.
4. Yologlu Z, Aydin H, Alp NA, Aribas BK, Kizilgoz V, Arda K. Diffusion weighted magnetic resonance imaging in the diagnosis of parotid masses. Preliminary results. *Saudi Med J*. 2016;37(12):1412-1416. [CrossRef]
5. Wang CW, Chu YH, Chiu DY, et al. JOURNAL CLUB: The Warthin tumor score: a simple and reliable method to distinguish Warthin tumors from pleomorphic adenomas and carcinomas. *AJR*. 2018;210(6):1330-1337. [CrossRef]
6. Inarejos Clemente EJ, Navallas M, Tolend M, et al. Imaging evaluation of pediatric parotid gland abnormalities. *RadioGraphics*. 2018;38(5):1552-1575. [CrossRef]
7. Motoori K, Yamamoto S, Ueda T, et al. Inter- and intratumoral variability in magnetic resonance imaging of pleomorphic adenoma: an attempt to interpret the variable magnetic resonance findings. *J Comput Assist Tomogr*. 2004;28(2):233-246. [CrossRef]
8. Matsushima N, Maeda M, Takamura M, Takeda K. Apparent diffusion coefficients of benign and malignant salivary gland tumors. Comparison to histopathological findings. *J Neuroradiol*. 2007;34(3):183-189. [CrossRef]

9. Matsusue E, Fujihara Y, Matsuda E, et al. Vanishing parotid tumors on MR imaging. *Yonago Acta Med*. 2018;61(1):33-39. [CrossRef]
10. Habermann CR, Arndt C, Graessner J, et al. Diffusion-weighted echo-planar MR imaging of primary parotid gland tumors: is a prediction of different histologic subtypes possible? *AJNR Am J Neuroradiol*. 2009;30(3):591-596. [CrossRef]
11. Thielker J, Grosheva M, Ihrler S, Wittig A, Guntinas-Lichius O. Contemporary management of benign and malignant parotid tumors. *Front Surg*. 2018;5:39. [CrossRef]
12. Awan MS, Ahmad Z. Diagnostic value of fine needle aspiration cytology in parotid tumors. *JMPA*. 2020;54:617-619.
13. Coulter M, Liu J, Marzouk M. Leiomyosarcoma ex pleomorphic adenoma of the parotid gland: a case report and literature review. *Case Rep Otolaryngol*. 2016;2016:9795785. [CrossRef]
14. Metwally Abo El Atta M, Ahmed Amer T, Mohamed Gaballa G, Tharwat Mohammed El-Sayed N. Multi-phasic CT versus dynamic contrast enhanced MRI in characterization of parotid gland tumors. *Egypt J Rad Nucl Med*. 2016;47(4):1361-1372. [CrossRef]
15. Khamis MEM, Ahmed AF, Ismail EI, Bayomy MF, El-Anwar MW. The diagnostic efficacy of apparent diffusion coefficient value and choline/creatine ratio in differentiation between parotid gland tumors. *Egypt J Rad Nucl Med*. 2018;49(2):358-367. [CrossRef]
16. Yerli H, Agildere AM, Aydin E, et al. Value of apparent diffusion coefficient calculation in the differential diagnosis of parotid gland tumors. *Acta Radiol*. 2007;48(9):980-987. [CrossRef]
17. Matsusue E, Fujihara Y, Matsuda E, et al. Differentiating parotid tumors by quantitative signal intensity evaluation on MR imaging. *Clin Imaging*. 2017;46:37-43. [CrossRef]
18. Gatidis S, Graf H, Weiß J, et al. Diffusion-weighted echo planar MR imaging of the neck at 3 T using integrated shimming: comparison of MR sequence techniques for reducing artifacts caused by magnetic-field inhomogeneities. *Magma*. 2017;30(1):57-63. [CrossRef]
19. Srivastava A, Wang J, Zhou H, Melvin JE, Wong DT. Age and gender related differences in human parotid gland gene expression. *Arch Oral Biol*. 2008;53(11):1058-1070. [CrossRef]
20. Direk FK, Deniz M, Uslu AI, Doğru S. Anthropometric analysis of orbital region and age-related changes in adult women. *J Craniofac Surg*. 2016;27(6):1579-1582. [CrossRef]
21. Yerli H, Aydin E, Haberal N, Harman A, Kaskati T, Alibek S. Diagnosing common parotid tumours with magnetic resonance imaging including diffusion weighted imaging vs fine-needle aspiration cytology. *Dentomaxillofac Radiol*. 2010;39(6):349-355. [CrossRef]
22. Tartaglione T, Botto A, Sciandra M, et al. Differential diagnosis of parotid gland tumours: which magnetic resonance findings should be taken in account? *Acta Otorhinolaryngol Ital*. 2015;35(5):314-320. [CrossRef]
23. Srinivasan A, Dvorak R, Perni K, Rohrer S, Mukherji SK. Differentiation of benign and malignant pathology in the head and neck using 3T apparent diffusion coefficient values: early experience. *AJNR Am J Neuroradiol*. 2008;29(1):40-44. [CrossRef]
24. Keil B, Blau JN, Biber S, et al. A 64-channel 3T array coil for accelerated brain MRI. *Magn Reson Med*. 2013;70(1):248-258. [CrossRef]
25. Tao X, Yang G, Wang P, et al. The value of combining conventional, diffusion-weighted and dynamic contrast-enhanced MR imaging for the diagnosis of parotid gland tumours. *Dentomaxillofac Radiol*. 2017;46(6):20160434. [CrossRef]
26. Yeh CK, Johnson DA, Dodds MW. Impact of aging on human salivary gland function: a community-based study. *Aging (Milano)*. 1998;10(5):421-428. [CrossRef]
27. Wang J, Takashima S, Takayama F, et al. Head and neck lesions: characterization with diffusion-weighted echo-planar MR imaging. *Radiology*. 2001;220(3):621-630. [CrossRef]
28. Yazici D, Guney Z, Coktu MY, Yildirim I, Arikan OK. Clinicopathological analysis of parotid masses: six-year experience of a tertiary center. *J Pak Med Assoc*. 2020;70(2):308-312. [CrossRef]
29. Verhappen MH, Pouwels PJ, Ljumanovic R, et al. Diffusion-weighted MR imaging in head and neck cancer: comparison between half-Fourier acquired single-shot turbo spin-echo and EPI techniques. *AJNR Am J Neuroradiol*. 2012;33(7):1239-1246. [CrossRef]
30. Okahara M, Kiyosue H, Hori Y, Matsumoto A, Mori H, Yokoyama S. Parotid tumors: MR imaging with pathological correlation. *Eur Radiol*. 2003;13(suppl 4):L25-L33. [CrossRef]
31. Nikitakis NG, Tosios KI, Papanikolaou VS, Rivera H, Papanicolaou SI, Ioffe OB. Immunohistochemical expression of cytokeratins 7 and 20 in malignant salivary gland tumors. *Mod Pathol*. 2004;17(4):407-415. [CrossRef]
32. Jha V, Kolte S, Goyal S. Osteosarcoma arising in carcinosarcoma de novo parotid gland in a young man: an unusual case with review of literature. *J Clin Diagn Res*. 2017;11:8-10. [CrossRef]
33. İncİ E, Hocaoğlu E, Kılıckesmez Ö, Aydin S, Cİmİllİ T. Quantitative diffusion-weighted MR imaging in the differential diagnosis of parotid gland tumors: is it a useful technique? *Turkiye Klinikleri J Med Sci*. 2010;30(4):1339-1345. [CrossRef]
34. Alkan EO, Sarı L, Balsak S, Celik Yabul FC, Altıntaş F, Çoban G. Investigation of the correlation between preoperative diffusion tensor imaging parameters and histopathological findings in patients with meningioma. *Curr Res MRI*. 2022;1(1):15-17. [CrossRef]
35. Teh A, Aswin Kumar A, Teh C, et al. Overview of parotid gland masses. J am osteopath Coll Radiol. 2018;7:5-10.
36. Qian W, Xu XQ, Zhu LN, et al. Preliminary study of using diffusion kurtosis imaging for characterizing parotid gland tumors. *Acta Radiol*. 2019;60(7):887-894. [CrossRef]